Supplementary Information for

Hierarchical P-ZSM-5 zeolites *in-situ* synthesized by home-made asymmetric quaternaryphosphonium for methanol-to-propylene

Yonglin Ren,[ab] Yimin Zhang,[ab] Xinyu Xu,[ab] Binbin He,[c] and Yun Zu*[ab]

[a] Faculty of Chemical Engineering, Kunming University of Science and Technology, Kunming 650500, P. R. China.

[b] Yunnan Provincial Key Laboratory of Energy Saving in Phosphorus Chemical Engineering and New Phosphorus Materials, Yunnan Technological Innovation Center of Phosphorus Resources, Kunming 650500, P. R. China.

[c] Faculty of Environmental Science and Engineering, Kunming University of Science and Technology, Kunming 650500, P.R. China.

*Corresponding author.

E-mail address:

zuyun1990@126.com (Y. Zu)

Table of contents

Experimental Procedures Section

Characterization

Inductively coupled plasma-optical emission spectrometer (ICP-OES). ICP-OES (Agilent 5800) analysis was used to measure the contents of silicon, aluminum, and phosphorus elements in the as-prepared zeolite samples.

Ion-selective electrode (ISE). The fluoride concentration was determined by the standard method using an ion-selective electrode. Under neutral conditions, the electrode potential of the solution was measured directly using a saturated glycury electrode as a reference electrode.

X-ray diffraction (XRD). XRD measurements of the samples were performed on a Bruker D8 Advance diffractometer using Cu Kα radiation working at tube voltage of 40 kV and tube current of 40 mA. The scanning step size was 0.02°, and the scanning range was 5-90°. The XRD pattern from the powder sample was recorded at ambient conditions.

Calculation of relative crystallinity. The relative crystallinity of the zeolite samples was calculated based on the integration of the peak areas of the characteristic peaks at 22.5-25^{o} of their XRD patterns; the sample with the largest peak area obtained by integration at 22.5-25^{o} was considered to have a relative crystallinity of 100%, and the rest of the samples was compared with it to obtain the relative crystallinity. The specific calculation formula was as follows:

$$R = A_i/A_{max} \times 100\%$$

where, R was the relative crystallinity of the sample, A_i was the peak area obtained by integrating the XRD pattern of the sample at 22.5-25^{o}, and A_{max} was the maximum peak area in the sample.

N_2 sorption. The Brunauer-Emmett-Teller (BET) surface areas and pore volume of the samples were determined from N_2 adsorption-desorption isotherms at -196 ^oC recorded on an Autorsorb-IQ-3MP instrument (Quantachrome). Prior to the measurements, the samples were degassed under an evacuated atmosphere at 350 ^oC for 6 h.

Scanning electron microscopy (SEM). The morphology of zeolites was investigated by scanning electron microscopy (SEM) images on a Nova-Nano450 instrument, where the samples were dispersed by sonication in ethanol for ten minutes prior to the experiment.

High resolution transmission electron microscopy (HRTEM). High resolution transmission electron microscopy (HRTEM), high angle annular dark field-scanning transmission electron microscopy (HAADF-STEM), and energy-dispersive X-ray (EDX) elemental mapping images were performed on a JEOL-2100F instrument. The accelerating voltage was 200 kV. The samples were prepared by suspending the sample powder in ethanol and then dropping the suspension onto a copper grid.

Solid-state magic-angle-spinning (MAS) NMR measurements. The solid-state MAS NMR studies of zeolites were carried out on a Bruker Avance III 400WB spectrometer with one-dimensional ^{27}Al and ^{31}P nuclei resonating at 104.3 and 161.9 MHz, respectively. Prior to the NMR measurements, the samples were dehydrated in a vacuum at 400 ^oC (at pressures lower than 10^{-2} Pa) for 10 h. The samples were then cleaned in a glove box with dry nitrogen. The materials were then sealed and stored in glass tubes until they were transferred to a gas-tight state, and then the MAS NMR rotor was cleaned with dry nitrogen in a glove box. The NMR experiments were performed using a single-pulse excitation of 6.5 μs and a cyclic delay of 4 s with a rotational frequency of 10 kHz.

In-situ Fourier transform infrared (FTIR) measurements. To track hydroxyl changes during the reassembly process, *in-situ* FTIR spectroscopy was performed on a BRUKER VERTEX 70 spectrometer equipped with a self-made high-temperature reaction chamber. Prior to the experiment, 15 mg of dry sample wafers were loaded into the *in-situ* cell and pretreated at 150 ^{o}C for 1 h in a high purity nitrogen atmosphere. The temperature was then gradually increased to 550 ^{o}C at a rate of 2 ^{o}C/min for 2 h. The signals were collected continuously during the process in the range of 4000-1200 cm^{-1} with a resolution of 4 cm^{-1}.

Pyridine-dosing FTIR (Py-FTIR) measurements. The acidic type and strength of the as-prepared samples were studied by *in-situ* FTIR spectroscopy with pyridine as a probing molecule. The supporting wafer (10~12 mg/cm^2) of sample was activated in the *in-situ* IR cell with CaF_2 at 400 ^{o}C for 4 h under high vacuum (< 10^{-3} Pa) and cooled down to 150 ^{o}C. The activated wafer was, then, exposed to pyridine vapor at 150 ^{o}C for 0.5 h, followed by the desorption of saturated adsorbed samples at 150 and 400 ^{o}C for 1 h, respectively. The final spectra at different temperatures were scanned in the range of 4000-1200 cm^{-1} by collecting 32 scans at a resolution of 4 cm^{-1}.

NH_3-temperature programmed desorption (NH_3-TPD). NH_3-TPD measurements were performed on a BSD-Chem C200 analyzer. Before the adsorption, the sample (150 mg) was activated in flowing He (30 $mL{\cdot}min^{-1}$) at 400 ^{o}C for 3 h. Adsorption of gas mixture NH_3 (10%)-He (90%) until saturation took place at 120 ^{o}C, the sample was, then, flushed with flowing He (30 $mL{\cdot}min^{-1}$) at the same temperature until stable baseline condition. TPD measurements were done from 120 to 800 ^{o}C with a heating rate of 10 $^{o}C{\cdot}min^{-1}$, with He (30 $mL{\cdot}min^{-1}$) as the carrier gas. The amount of desorbed ammonia was detected by a thermal conductive detector.

Gas chromatography - mass spectrometer (GC-MS). Retained hydrocarbons soluble in CH_2Cl_2 were extracted by dissolving 20 mg of spent catalysts with a given fraction in 1 mL 40% HF for 3 h. After neutralization (pH = 7) with 2 M NaOH, 6 mL CH_2Cl_2 was added to a Teflon beaker to extract the organic compounds trapped within spent catalysts. Then, soluble and insoluble coke species were separated by separatory funnel. The mixing of soluble and insoluble coke species was oscillated with ultrasonic for 3 h. Finally, soluble coke species were obtained by filtration and concentrated to 0.8 ~ 1 mL, and then analyzed by GC-MS (Agilent 7890A/5975C) equipped with a chromatographic column HP-5ms (30 m × 0.250 mm × 0.25 μm), respectively. For analysis condition of the products, the column temperature program was set from 50 to 120 ^oC with temperature rate 10 $^oC \cdot min^{-1}$, and hold 2 min at 120 ^oC, and subsequently, from 120 to 280 ^oC with heating rate 3 $^oC \cdot min^{-1}$, kept 2 min at 280 ^oC. The injection volume was 3 μL.

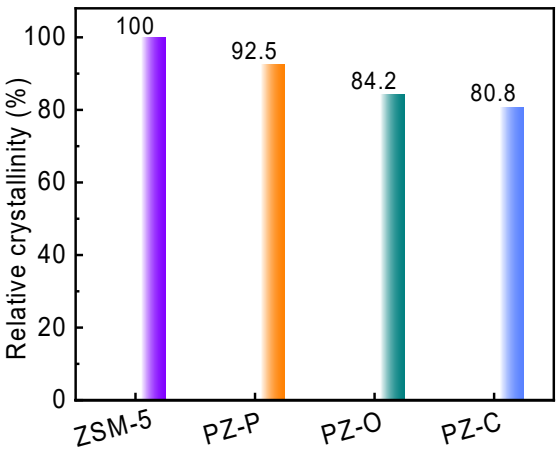

Figure S1. Relative crystallinity of as-prepared zeolite samples.

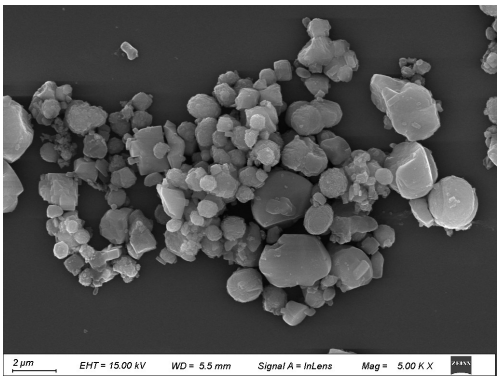

Figure S2. SEM image of as-prepared ZSM-5 zeolite sample.

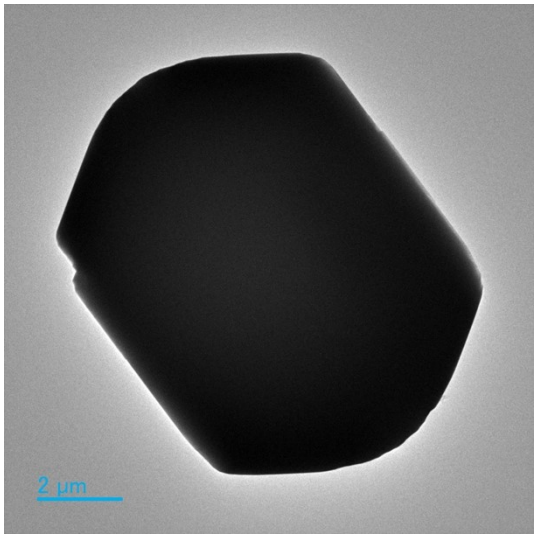

Figure S3. HRTEM image of as-prepared ZSM-5 zeolite sample.

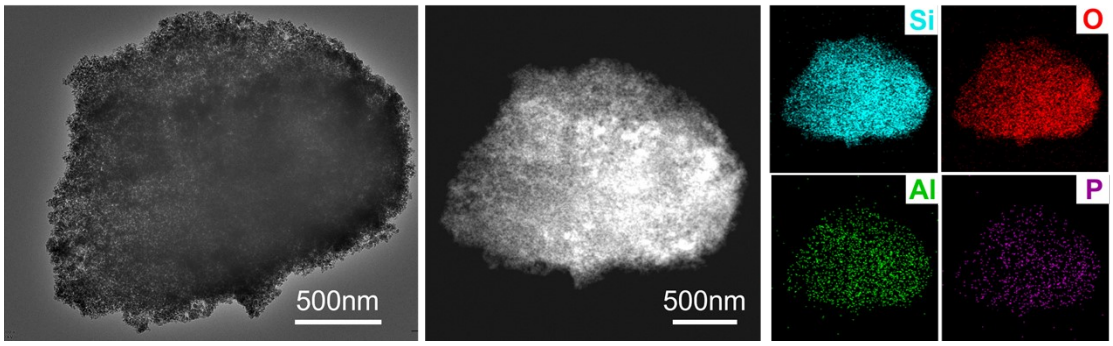

Figure S4. HRTEM, HADDF-STEM, and EDX element (Si, O, Al, and P) mapping images of hierarchical PZ-O zeolite.

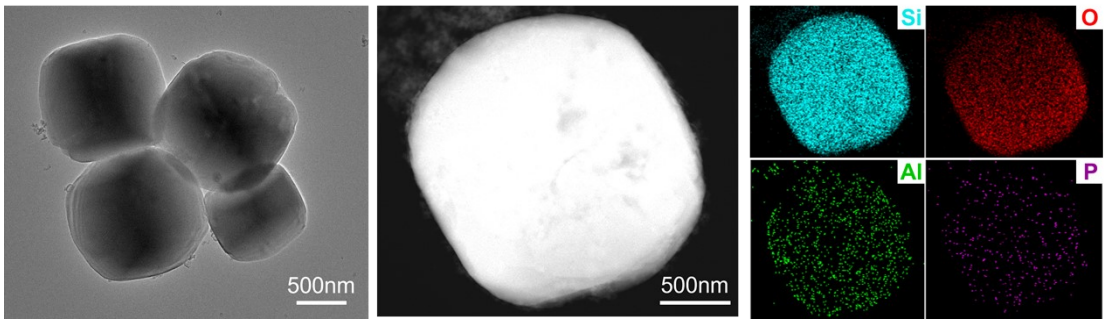

Figure S5. HRTEM, HADDF-STEM, and EDX element (Si, O, Al, and P) mapping images of hierarchical PZ-C zeolite.

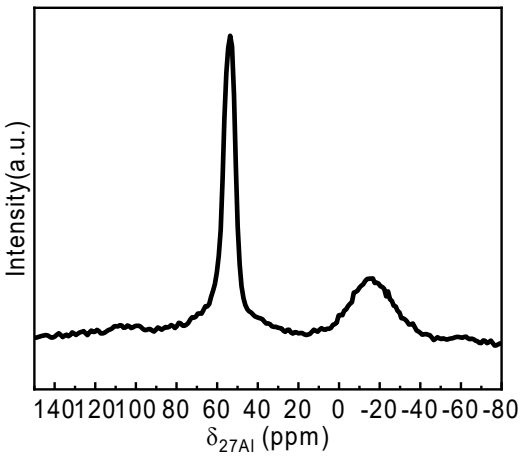

Figure S6. ^{27}Al MAS NMR spectra of as-prepared ZSM-5 zeolite sample.

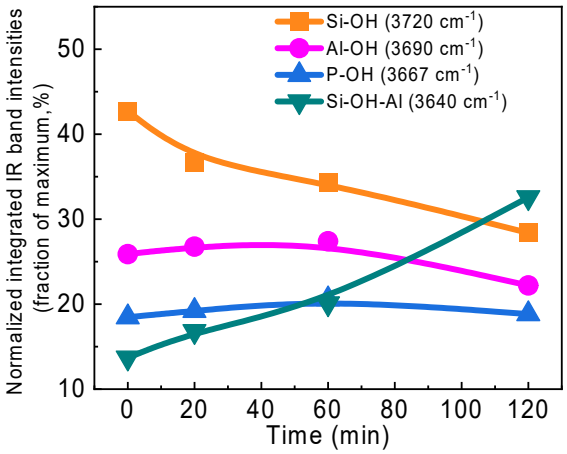

Figure S7. Time-dependence of the ratio of the integrated intensities of the bands at 3720, 3690, 3667 and 3640 cm^{-1} for the PZ-P zeolite sample during *in-situ* calcination as the system temperature up to 550 °C.

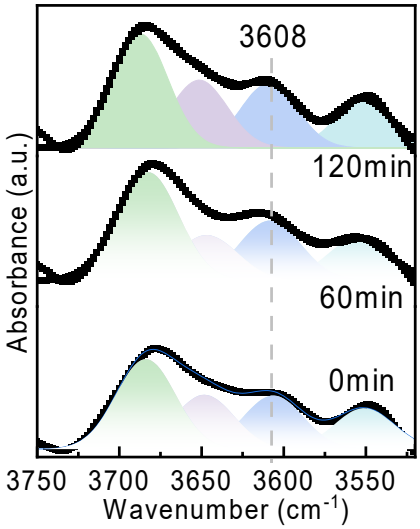

Figure S8. *In-situ* hydroxyl FTIR spectra of ZSM-5 zeolite with the template TPAOH during the calcination process at air atmosphere.

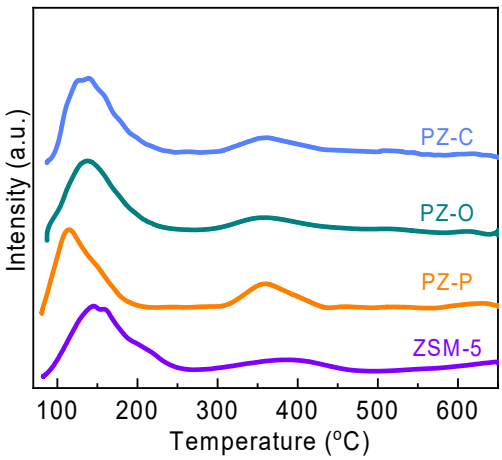

Figure S9. NH_3-TPD profiles of ZSM-5 and hierarchical P-ZSM-5 zeolite samples.

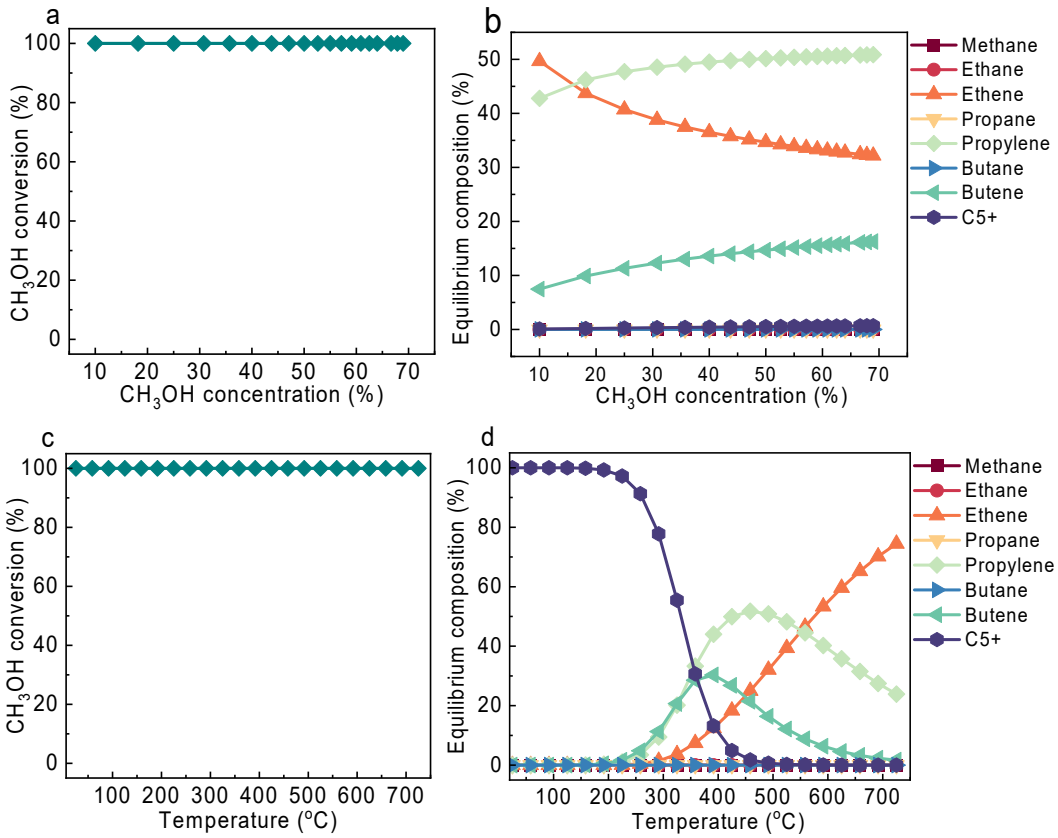

Figure S10. (a, c) CH_3OH equilibrium conversion, and (b, d) Product equilibrium composition obtained from HSC 6.0 calculations.

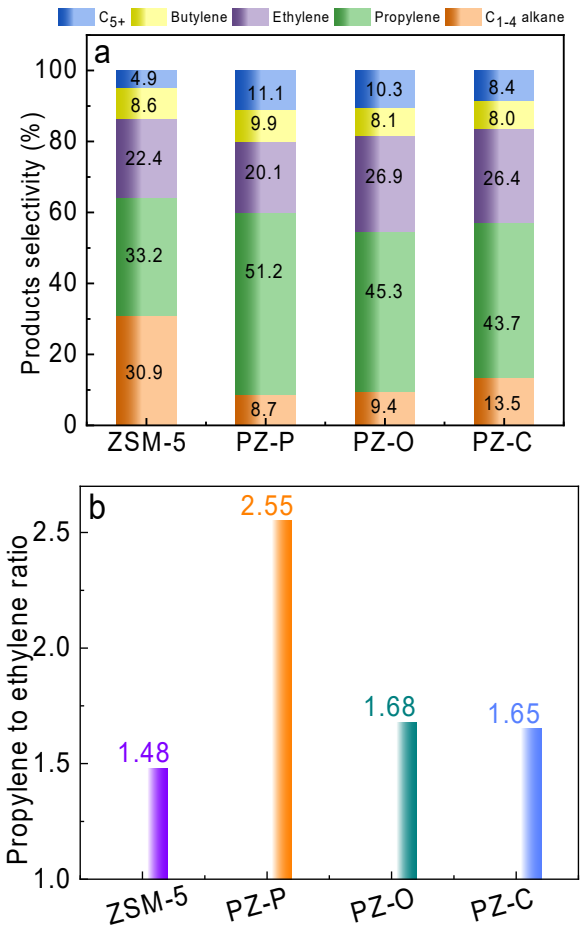

Figure S11. (a) Products selectivity and (b) Propylene to ethylene ratio during the MTP reaction over the zeolite catalysts for reaction 1 h. Reaction conditions: T = 480 ^{o}C, 1 atm, WHSV = 6 h^{-1}, catalyst weight = 100 mg.

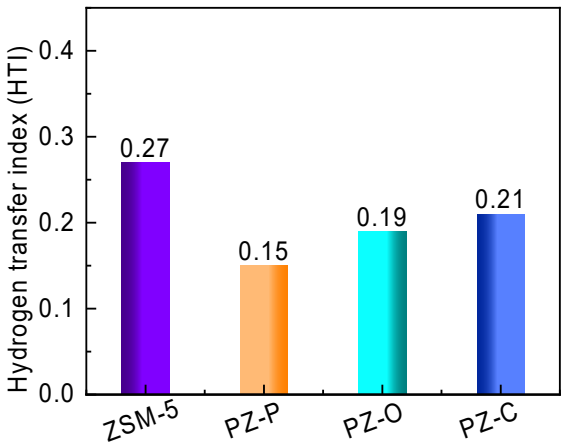

Figure S12. Hydrogen transfer index (HTI) of different zeolites in MTP reaction for 1.0 h.

Note: Hydrocarbon transfer indexes (HTI) are calculated according to the yield of C4 alkanes to that for C4 alkenes and C4 alkanes.

Table S1. Elemental contents of Si, Al, P and F in the zeolite samples.

Samples	Si (wt.%)	Al (wt.%)	P (wt.%)	F (wt.%)	Si/Al	P/Al
ZSM-5	51.89	0.71	--	0.002	70.47	--
PZ-P	36.06	0.50	0.59	0.002	69.54	1.02
PZ-O	34.83	0.52	0.57	0.004	64.58	0.95
PZ-C	34.82	0.54	0.62	0.003	62.18	1.00

Table S2. Pore structural properties of different zeolite samples.

Samples	S_{BET} (m^2/g) [a]	S_{mic} (m^2/g) [b]	S_{ext} (m^2/g) [b]	V_{total} (cm^3/g) [c]	V_{mic} (cm^3/g) [c]	V_{meso} (cm^3/g) [d]
ZSM-5	423.2	398.8	24.4	0.21	0.17	0.04
PZ-P	352.4	193.7	158.7	0.22	0.12	0.10
PZ-O	353.1	182.6	170.5	0.21	0.09	0.12
PZ-C	353.6	147.3	206.3	0.20	0.07	0.13

[a] Measured by BET method;

[b] Measured by *t*-plot method;

[c] Volume adsorbed at P/P_0=0.99;

[d] Mesopore volumes calculated by V_{total}-V_{micro}.

Table S3. Acid properties of as-prepared zeolite samples obtained by pyridine-dosing FTIR measurements.

Samples	Brønsted acid amount ($\mu mol \cdot g^{-1}$)		Lewis acid amount ($\mu mol \cdot g^{-1}$)	
	150 °C	400 °C	150 °C	400 °C
ZSM-5	225.5	67.3	49.5	6.7
PZ-P	175.9	95.3	36.1	9.2
PZ-O	173.3	85.5	38.5	5.3
PZ-C	170.1	73.8	35.7	3.4

Note: The area of peak was defined as the total acid amount after degassed at 150 °C and defined as the strong acid amount after degassed at 400 °C. The difference value between the total acid amount and the strong acid amount was the weak acid amount.

Table S4. Comparison of catalyst reaction stability and product selectivity for the MTP reaction.

Catalysts	Si/Al ratio	WHSV (h^{-1})	Temperature (°C)	Lifetime (h)	C_3H_6 selectivity (%) [a]	Olefins selectivity (%) [a]	P/E	Ref.
H-SPP-Bu-DMPy	38	1.0	480	160.0	48.5	84.5	2.5	S1
ProSeed-Z5-1	120	12.5	470	18.0	52.7	82.1	3.6	S2
ZSM-5 nanocages	62	3.8	450	60.3	36.9	73.6	2.5	S3
HZSM-5 (0.027/1)	37	0.2	400	2.0	31.0	68.0	1.7	S4
Z100	97	5.0	450	20.0	36.4	71.9	2.5	S5
SFD-ZSM-5-0.8-16	--	18	400	47.0	35.0	69.4	3.7	S6
SA-34-II-P-S	--	1.0	425	7.5	43.9	89.9	--	S7
DDR_172*	168	--	400	--	50.6	86.7	1.9	S8
S-HZ-0.1AT	79	6	450	120	50.2	79.5	--	S9
S18-HPP	--	2	400	2.5	42.5	85.2	--	S10
SAPO-34	--	1.0	400	8.3	40.8	83.5	--	S11
ZEOS	--	6.6	450	3.0	37.0	87.0	0.7	S12
PZ-P	75	6.0	480	23.0	51.2	81.2	2.6	This work

--: Data not available.

[a] Selectivity calculated as the reaction reaches stabilization.

References

[S1] Y. Ma, X. Tang, J. Hu, Y. Ma, W. Chen, Z. Liu, S. Han, C. Xu, Q. Wu, A. Zheng, L. Zhu, X. Meng, F.-S. Xiao, Design of a small organic template for the synthesis of self-pillared pentasil zeolite nanosheets, J. Am. Chem. Soc. 144 (2022) 6270-6277.
[S2] Y. Liu, Q. Zhang, J. Li, X. Wang, O. Terasaki, J. Xu, J. Yu, Protozeolite-seeded synthesis of single-crystalline hierarchical zeolites with facet-shaped mesopores and their catalytic application in methanol-to-propylene conversion, Angew. Chem. Int. Ed. 134 (2022).
[S3] G. Chen, J. Li, S. Wang, J. Han, X. Wang, P. She, W. Fan, B. Guan, P. Tian, J. Yu, Construction of single-crystalline hierarchical ZSM-5 with open nanoarchitectures via anisotropic-kinetics transformation for the methanol-to-hydrocarbons reaction, Angew. Chem. Int. Ed. 134 (2022) e202200677.
[S4] L. Lin, M. Fan, A.M. Sheveleva, X. Han, Z. Tang, J.H. Carter, I. da Silva, C.M.A. Parlett, F. Tuna, E.J.L. McInnes, G. Sastre, S. Rudić, H. Cavaye, S.F. Parker, Y. Cheng, L.L. Daemen, A.J. Ramirez-Cuesta, M.P. Attfield, Y. Liu, C.C. Tang, B. Han, S. Yang, Control of zeolite microenvironment for propene synthesis from methanol, Nat. Commun. 12 (2021) 822..
[S5] Y. Xue, J. Li, P. Wang, X. Cui, H. Zheng, Y. Niu, M. Dong, Z. Qin, J. Wang, W. Fan, Regulating Al distribution of ZSM-5 by Sn incorporation for improving catalytic properties in methanol to olefins, Appl. Catal. B: Environ. 280 (2021) 119391.
[S6] Y. Zhang, K. Zhang, C. Shang, X. Wang, L. Wu, G. Huang, H. Wang, Q. Sun, X.D. Chen, Z. Wu, Synthesis of hierarchical ZSM-5 microspheres with superior performance for catalytic methanol-to-olefin conversion, AIChE J. 69 (2023) e17913.
[S7] C. Wang, L. Yang, M. Gao, X. Shao, W. Dai, G. Wu, N. Guan, Z. Xu, M. Ye, L. Li, Directional construction of active naphthalenic species within SAPO-34 crystals toward more efficient methanol-to-olefin conversion, J. Am. Chem. Soc. 144 (2022) 21408–21416.
[S8] J. Hua, X. Dong, J. Wang, C. Chen, Z. Shi, Z. Liu, Y. Han, Methanol-to-olefin conversion over small-pore DDR zeolites: Tuning the propylene selectivity via the olefin-based catalytic cycle, ACS Catal. 10 (2020) 3009–3017.
[S9] J. Li, H. Ma, Y. Chen, Z. Xu, C. Li, W. Ying, Conversion of methanol to propylene over hierarchical HZSM-5: The effect of Al spatial distribution, Chem. Commun. 54 (2018) 6032–6035.
[S10] M. Wen, L. Ren, J. Zhang, J. Jiang, H. Xu, Y. Guan, P. Wu, Designing SAPO-18 with energetically favorable tetrahedral Si ions for an MTO reaction, Chem. Commun. 57 (2021) 5682–5685.
[S11] L. Yang, C. Wang, L. Zhang, W. Dai, Y. Chu, J. Xu, G. Wu, M. Gao, W. Liu, Z. Xu, P. Wang, N. Guan, M. Dyballa, M. Ye, F. Deng, W. Fan, L. Li, Stabilizing the framework of SAPO-34 zeolite toward long-term methanol-to-olefins conversion, Nat. Commun. 12 (2021) 4661.
[S12] J. Zhou, M. Gao, J. Zhang, W. Liu, T. Zhang, H. Li, Z. Xu, M. Ye, Z. Liu, Directed transforming of coke to active intermediates in methanol-to-olefins catalyst to boost light olefins selectivity, Nat. Commun. 12 (2021) 17.